



FEATURE ARTICLE

Estimating North Atlantic right whale prey based on *Calanus finmarchicus* thresholds

Camille H. Ross^{1,2,*}, Jeffrey A. Runge², Jason J. Roberts³, Damian C. Brady², Benjamin Tupper¹, Nicholas R. Record¹

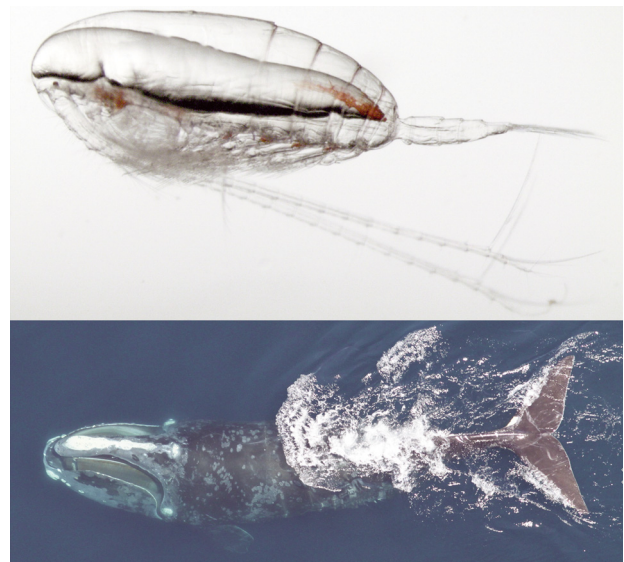
¹Tandy Center for Ocean Forecasting, Bigelow Laboratory for Ocean Sciences, East Boothbay, ME 04544, USA

²Darling Marine Center, University of Maine, School of Marine Sciences, Walpole, ME 04573, USA

³Marine Geospatial Ecology Laboratory, Duke University, Durham, NC 27708, USA

ABSTRACT: The planktonic copepod *Calanus finmarchicus* is a fundamental prey resource for the critically endangered North Atlantic right whale *Eubalaena glacialis*. Incorporation of prey information into *E. glacialis* decision support tools could improve management. Zooplankton time series are usually analyzed with respect to abundance, but predators such as *E. glacialis* forage based on whether prey aggregations exceed energetic thresholds. In order to better understand the distribution and dynamics of the high-abundance end of *C. finmarchicus* on the northeastern US continental shelf, where *E. glacialis* feed, we modeled the environmental conditions associated with *C. finmarchicus* densities that exceed nominal feeding thresholds. Threshold values were chosen based on a review of *E. glacialis* feeding behavior throughout the domain. Following model selection procedures, we used a random forest model with bathymetry, bottom temperature, bottom salinity, day of year, sea surface temperature, sea surface temperature gradient, bathymetric slope, time-integrated chlorophyll, current velocity gradient, and wind covariates. Model performance was highest with thresholds that matched reported *E. glacialis* feeding thresholds equivalent to 10 000 copepods m⁻². The high-density aggregations of *C. finmarchicus* had some different covariate responses compared to previous statistical abundance models, such as a warmer temperature range at both the surface and at depth, as well as a much higher degree of spatial variability. The output data layers of the model are designed to link with *E. glacialis* models used in US governmental decision support tools. Including this type of foraging information in decision support tools is a step forward in managing this critically endangered species.

KEY WORDS: *Calanus finmarchicus* · *Eubalaena glacialis* · Habitat modeling · Prey density



A novel modeling approach looking at prey densities through the lens of right whale feeding has potential to aid conservation.

Photos: *C. finmarchicus*, Cameron R. S. Thompson; Right whale, NOAA/NEFSC/Christin Khan (MMPA Permit #17355)

1. INTRODUCTION

Calanus finmarchicus, a species of planktonic copepod, is foundational in the subarctic Northwest Atlantic ecosystem (Pershing & Stamieszkin 2020). It serves as a fundamental prey resource for a wide range of species in higher trophic levels, including the critically endangered North Atlantic right whale *Eubalaena glacialis* (listed as 'Critically Endangered' on the IUCN Red List) (Cooke 2020). Management strategies to conserve *E. glacialis* rely on models that forecast habitat use, especially foraging areas (Meyer-Gutbrod

*Corresponding author: cross@bigelow.org

et al. 2021). *E. glacialis* are observed in areas with dense *C. finmarchicus* aggregations (Wishner et al. 1988, 1995, Murison & Gaskin 1989, Mayo & Marx 1990, Kenney & Wishner 1995, Baumgartner & Mate 2003, Baumgartner et al. 2003, Jiang et al. 2007) and they appear to select these areas based on whether abundances are above a critical feeding threshold (Mayo & Marx 1990, Kenney & Wishner 1995). While considerable research has been devoted to understanding the abundance and distribution patterns of *C. finmarchicus* (e.g. Wishner et al. 1988, Kann & Wishner 1995, Meise & O'Reilly 1996, Lynch et al. 1998, Pershing et al. 2009a, Ji 2011, Reygondeau & Beaugrand 2011, Record et al. 2013, 2018, Chust et al. 2014, Melle et al. 2014, Runge et al. 2015, Ji et al. 2017, Sorochan et al. 2019), far fewer studies have focused on the distribution of foraging habitat with prey densities above a feeding threshold (e.g. Pendleton et al. 2012, Plourde et al. 2019).

The need for predictive skill is evident in ongoing management challenges in both the USA and Canada (Record et al. 2019, Meyer-Gutbrod et al. 2021). For example, sea surface and bottom temperatures in the Gulf of Maine have been warming rapidly, particularly between 2005 and 2015 (Pershing et al. 2015, Record et al. 2019, Friedland et al. 2020, Gonçalves Neto et al. 2021). While species distribution models have estimated a gradual northeastward shift of 8.1 km per decade in the distribution of *C. finmarchicus* (Chust et al. 2014), abrupt shifts occurring within the past decade outpace these projections, and distributions have large regional variation (Ji et al. 2022). Changes in the Gulf Stream drove an abrupt shift to warmer temperatures in the deep waters entering the Gulf of Maine beginning in 2008 (Gonçalves Neto et al. 2021), which caused a decline in *C. finmarchicus* abundance in the eastern Gulf of Maine by 2010 (Record et al. 2019). *E. glacialis* responded by shifting from the eastern Gulf of Maine to the Gulf of St. Lawrence to forage in summer, resulting in unforeseen mortality due to entanglements and ship strikes. The resulting shifts in right whale foraging and, consequently, population growth have put the viability of the species in question (Kraus et al. 2016, Davis et al. 2017). Improved prediction could help management be more adaptive to such abrupt shifts in foraging habitat (Davies & Brillant 2019). Examples of more adaptive management could include directing future survey effort and aiding in longer term planning.

The accuracy of *E. glacialis* habitat-use models can be improved by the inclusion of a prey field (e.g. Pendleton et al. 2012), highlighting the importance of developing a suitable prey field for use as input to these models. A

coupled biophysical model of the *C. finmarchicus* life cycle and abundance in the western Gulf of Maine sufficiently simulated this species' phenology for use in a whale forecast (Pershing et al. 2009a,b). While previous modeling efforts have focused on *C. finmarchicus* abundance, they have not yet characterized the environmental conditions associated with the formation of high-density aggregations that influence *E. glacialis* foraging behavior. A focus on abundance tends to smooth out the extreme values that would describe high-density prey patches, as most skill metrics are optimized across the full abundance distribution. Generally, models are on spatial scales that are very coarse (e.g. Reygondeau & Beaugrand 2011) or use smoothed approaches, such as generalized additive models (Grieve et al. 2017), that are useful for looking at broad dynamics, but are not suitable for the extreme high values in the *C. finmarchicus* distribution that form *E. glacialis* feeding habitat. Essentially, it is the right-hand tail of the prey abundance distribution that matters for this type of foraging strategy, whereas most modeling approaches focus on the middle of the distribution.

Dense aggregations of *C. finmarchicus* in the Northwest Atlantic form by complex interactions among local production, predation, and external supply (Ji et al. 2022), individual behaviors, and physical oceanographic concentrating mechanisms (Wishner et al. 1988, Epstein & Beardsley 2001, Davies et al. 2014; reviewed by Sorochan et al. 2021). For most of the year, the primary prey resource for *E. glacialis* is *C. finmarchicus*. Additionally, the type of aggregation that *E. glacialis* may target also depends on the size composition of individual *C. finmarchicus*. In the Great South Channel, *E. glacialis* likely target aggregations of later stage *C. finmarchicus*, as opposed to targeting aggregations based on density alone (Kenney & Wishner 1995). These aggregations can last for several days and cover several square kilometers (Wishner et al. 1988).

Here we analyze *C. finmarchicus* distribution through the lens of *E. glacialis* foraging behavior on the northeastern US continental shelf using the concept of a feeding threshold: the prey aggregation density above which foraging becomes energetically advantageous for *E. glacialis*. Local high-density copepod aggregations are often described as 'patches' or 'swarms,' although there is no clear agreement on the level of abundance density that delineates one of these designations. Similarly, the magnitude of a feeding threshold for *E. glacialis* is not precisely known, and likely depends on internal factors, such as energetic needs and satiation level that vary with demographic stage (e.g. Miller et al. 2011, Fortune et

al. 2013), as well as external factors, such as prey species, developmental stage, energy density, vertical distribution, interannual and individual variability in lipid content at different developmental stages (for *C. finmarchicus*, in particular), and the prey potentially available elsewhere. We therefore took an approach where we constrained the problem with upper and lower bounds on the minimum abundance of individual *C. finmarchicus* required to constitute a high-density patch. We described patches using a hypothetical right whale feeding density threshold, τ . Then, we analyzed the sensitivity of the *C. finmarchicus* model output to 4 potential values of τ between those bounds obtained from the literature (see Table 2). To avoid confusion around terms such as ‘patchiness,’ we referred to these high-density aggregations as ‘ τ -patches.’

We empirically estimated the presence of *C. finmarchicus* τ -patches in excess of potential *E. glacialis* feeding thresholds. Based on an extensive literature review of field studies of feeding *E. glacialis*, we examined multiple feeding thresholds in order to classify the abundances of *C. finmarchicus* as patch or no-patch. We also identified the advantages and tested the limitations of statistical modeling approaches, specifically those of random forest models. The resulting modeled prey fields were designed for use as input to the North Atlantic right whale density surface model developed for use by the US Navy’s Atlantic Fleet Training and Testing (AFTT) Phase IV Environmental Impact Statement and the National Oceanic and Atmospheric Administration’s (NOAA’s) Atlantic Large Whale Take Reduction Team (i.e. the Duke right whale density surface model version 9: hereafter ‘right whale density model’) (Roberts et al. 2016, 2020) to examine potential management strategies, such as targeted closures and reduction of vertical lines. Beyond the utility of the prey fields, this study presents a novel approach to modelling and thinking about copepod data through the lens of predation.

2. MATERIALS AND METHODS

2.1. Study area

The study area was the northeastern US continental shelf from the Mid-Atlantic Bight to the eastern Gulf of Maine (Fig. 1). The study area included 2 critical habitat regions for *Eubalaena glacialis*: Cape Cod Bay (Mayo et al. 2004) and the Great South Channel (CETAP 1982, Kenney & Wishner 1995). We also chose to include Jordan Basin, Massachusetts

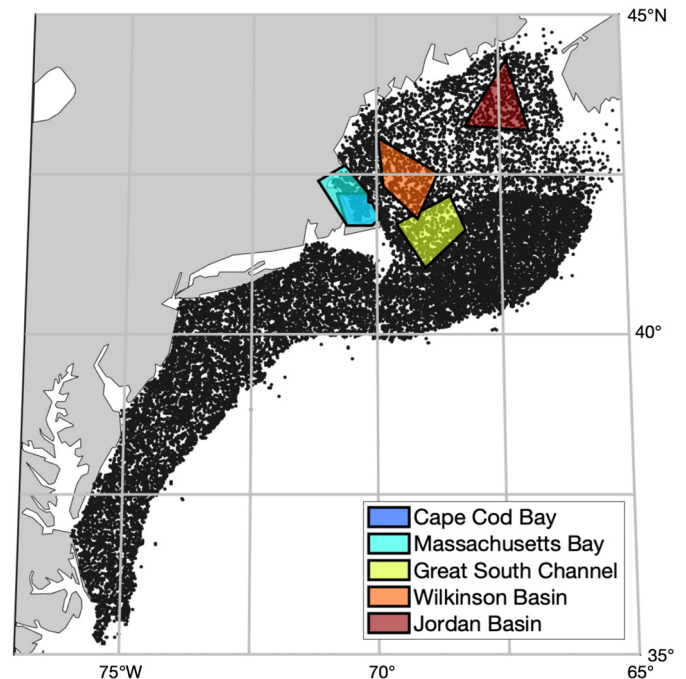


Fig. 1. Study area with critical habitat polygons for Cape Cod Bay and the Great South Channel, and potential habitats: Jordan Basin, Massachusetts Bay, and Wilkinson Basin. The Massachusetts Bay polygon is superimposed onto the Cape Cod Bay polygon due to geographic overlap. black points indicate the National Oceanic and Atmospheric Administration (NOAA) Fisheries Ecosystem Monitoring Program (MARMAP/EcoMon) survey stations from 2000 to 2017. Due to the randomly stratified sampling design, every station was likely only sampled once

Bay, and Wilkinson Basin, which are all important *Calanus finmarchicus* sampling locations (Fig. 1) (Pendleton et al. 2009). While we highlighted these specific regions for visualization and comparison, the model encompassed the domain used in the right whale density model.

2.2. Data sources

C. finmarchicus data were obtained from the NOAA Fisheries Ecosystem Monitoring Program (MARMAP/EcoMon) survey (<https://www.st.nmfs.noaa.gov/copepod/time-series/us-50101/>). Briefly, samples were collected using a 333 μ m mesh bongo net towed obliquely from the surface to 200 m depth, or the bottom in shallower regions (Kane 2007, Richardson et al. 2010). The mesh size is approximately equivalent to the estimated filtering efficiency of *E. glacialis* baleen (Mayo et al. 2001) and reflects the size groups with prosome lengths >1.5 mm that would likely be captured by whales (Lehoux et al.

2020). We used both the total *C. finmarchicus* abundance (denoted ‘unstaged’ here) captured by the net (predominantly stages C2 through adult), as well as the late stage abundance (C4 through adult). Abundance data were converted to absence or presence of a τ -patch (denoted by zero and one, respectively) based on whether or not the abundance measured in a sample was below or above the nominal feeding threshold, τ . Presences/absences of τ -patches were then examined for association with a set of environmental covariates, including sea surface temperature, bottom water temperature, sea surface salinity, bottom water salinity, wind, bathymetry, bathymetric slope, time-integrated surface chlorophyll, sea surface temperature gradient, current speed in the u and v direction, and day of year (DoY). Monthly environmental covariates were the same as those used in the right whale density model (Table 1) (Roberts et al. 2016, 2020). These monthly covariates reflect interannual variability across the time period of this modeling exercise, from 2000 to 2017. The derived covariates (i.e. time-integrated surface chlorophyll, current velocity gradient, sea surface temperature gradient) were produced from these fields using R (version 4.0.3; R Core Team 2021).

2.3. Modeling framework

We developed a *C. finmarchicus* τ -patch formation threshold approach to parameterize the model. This approach was derived from optimal foraging theory

(Stephens & Krebs 1986), where foragers make decisions about whether to stay and feed in a patch or search for a better patch based on metrics such as prey density. For *E. glacialis* foraging, this amounts to exploring different thresholds (τ) of copepod prey concentration. Copepods are sampled in a wide variety of ways, including nets (of various mesh sizes), optics, acoustics, surface measurements versus water column measurements, and at a range of spatial and temporal resolutions. The most widespread copepod measurements in our region are the water column net tows comprising the EcoMon dataset, reported as individuals (ind.) m^{-2} . Thus, as we estimated upper and lower reasonable and extreme bounds for τ , we converted to units of ind. m^{-2} —i.e. what would be sampled by a vertical tow. The challenge is that whales feed on high-density layers within a vertical tow. Suppose a vertical tow measured an ind. m^{-2} density of *C. finmarchicus*, C_2 : determining whether this is above or below a threshold, τ , depends on the proportion, p , of the profile that is concentrated into a dense layer, and the layer thickness, z . The prey resource available is then $C_3 = pC_2/z$, where the subscripts refer to density m^{-3} and m^{-2} , respectively. If we suppose a layer thickness of $z = 20$ m, for example, (cf. Baumgartner & Mate 2003), and $p = 0.7$, then a threshold of $\tau = 40\,000$ ind. m^{-2} , as reported in Record et al. (2019), corresponds to a feeding layer of 1400 ind. m^{-3} , similar to the values reported by others using these units (Table 2) (Murison & Gaskin 1989, Mayo & Marx 1990, Woodley & Gaskin 1996, Michaud & Taggart 2007). Physical and biological processes can concentrate

Table 1. Monthly mean environmental covariates used in the τ -patch model were obtained from the North Atlantic right whale density surface model developed for use by the US Navy’s Atlantic Fleet Training and Testing (AFTT) Phase IV Environmental Impact Statement and the National Oceanic and Atmospheric Administration’s (NOAA’s) Atlantic Large Whale Take Reduction Team (i.e. the Duke right whale density surface model version 9) (Roberts et al. 2016, 2020). The covariates used are listed below, along with product and corresponding website

Covariate(s)	Product	More information
Wind	Cross-Calibrated Multi-Platform (CCMP) Wind Vector Analysis Product Version 2	www.remss.com/measurements/ccmp/
Chlorophyll-a	Copernicus-GlobColour processor	https://resources.marine.copernicus.eu/?option=com_csw&task=results?option=com_csw&view=details&product_id=OCEANCOLOUR_GLO_CHL_L4_REP_OBSERVATIONS_009_082
Sea surface temperature, Bottom temperature, Sea surface salinity, Bottom salinity, Current velocity (u & v)	GOFS 3.1 Hybrid Coordinate Ocean Model (HYCOM) + Navy Coupled Ocean Data Assimilation (NCODA) Global 1/12° Analysis (GLBv0.08)	https://www.hycom.org/dataserver/gofs-3pt1/analysis
Bathymetry, Slope	SRTM30_PLUS bathymetry	https://topex.ucsd.edu/WWW_html/srtm30_plus.html

Table 2. Literature review for *Eubalaena glacialis*–*Calanus finmarchicus* aggregation thresholds. The table includes the literature source, corresponding *C. finmarchicus* density with respect to *E. glacialis* feeding, and any relevant notes about how the density was obtained. The abundance densities were converted to upper and lower bounds ($p = 1.0$ and $z = 1$ m and 20 m, respectively) of ind. m^{-2} measurements based on methods described in Section 2.3; where p represents the proportion of the profile that is concentrated into a dense layer and z represents the layer thickness

Source	<i>C. finmarchicus</i> density	Notes	Location	Lower bound ($z = 1$ m)	Upper bound ($z = 20$ m)
Baumgartner & Mate (2003)	Minimum 3600 m^{-3}	Based on linear regression model	Bay of Fundy, Scotian Shelf	3600 m^{-2}	72 000 m^{-2}
Baumgartner et al. (2017)	14 900 \pm 14 400 m^{-3}	Maximum late-stage abundance in upper 15 m of water column	Cape Cod Bay, Great South Channel, Stellwagen Bank, Bay of Fundy, Roseway Basin, Jeffreys Ledge	14 900 m^{-2}	29 8000 m^{-2}
Beardsley et al. (1996)	8.7 $\times 10^3$ to 4.1 $\times 10^4$ m^{-3}	First number is the mean for the MOCNESS approach. Second number is the mean for acoustic approach	Great South Channel	8700 m^{-2}	820 000 m^{-2}
Fortune et al. (2013)	6618 \pm 3481 m^{-3}		Bay of Fundy	6618 m^{-2}	132 360 m^{-2}
Fortune et al. (2013)	14 778 \pm 18 594 m^{-3}		Cape Cod Bay	14 778 m^{-2}	295 960 m^{-2}
Kenney et al. (1986)	3 $\times 10^5$ to 1 $\times 10^6$ m^{-3}	Minimum to feed on routinely for survival	Great South Channel	300 000 m^{-2}	20 000 000 m^{-2}
Mayo & Marx (1990)	6.54 $\times 10^3$ m^{-3} observed 1000 m^{-3} suggested in discussion	Density in regions with right whale presence	Cape Cod Bay	1000 m^{-2}	20 000 m^{-2}
Michaud & Taggart (2007)	900 m^{-3}	Minimum to define right whale habitat based on energy density	Bay of Fundy	900 m^{-2}	18 000 m^{-2}
Murison & Gaskin (1989)	832 to 1070 m^{-3}	Minimum to define right whale habitat. First estimate is 1983; second estimate is 1984	Bay of Fundy	832 m^{-2}	21 400 m^{-2}
Record et al. (2019)	40 000 m^{-2}	Minimum threshold for high right whale occupancy	Eastern Gulf of Maine	35 000 m^{-2}	45 000 m^{-2}
Wishner et al. (1988)	41 600 m^{-3}	Maximum abundance from MOCNESS tow near feeding right whales	Great South Channel	41 600 m^{-2}	832 000 m^{-2}
Wishner et al. (1995)	9749 m^{-3}	Near feeding right whales	Northern Great South Channel	9749 m^{-2}	194 980 m^{-2}
Woodley & Gaskin (1996)	1139 m^{-3}	Depth-averaged density	Bay of Fundy	1139 m^{-2}	22 780 m^{-2}

copepods into layers at least as thin as $z = 5$ m (Mayo & Marx 1990). To test the full sensitivity of the model to these assumptions, we set $p = 1$ and $z = 1$ m and 20 m. In practice, z is likely >1 m and $p < 1$, but testing the more extreme values (i.e. $z = 1$ m) gives a fuller understanding of the model behavior. We used these unlikely, extreme values only to compute the lower bound of the potential τ estimates suggested in the literature (i.e. $\tau = 1000$ ind. m^{-2}) (Mayo & Marx 1990). We then used these assumptions along with the literature review in Table 2 to select 2 intermediate values

between the extreme lower bound calculation and the threshold density from Record et al. (2019), which resulted in 4 potential density threshold estimates of $\tau = 1000, 4000, 10\,000,$ and $40\,000$ ind. m^{-2} (Fig. 2).

Models were trained on the EcoMon dataset. Random forest models were built using the *biomod2* package in R using 10 cross-validation folds with random 70% to 30% training to testing data splits (Thuiller et al. 2009, R Core Team 2021). Random forests are highly accurate predictive models (Li & Wang, 2013) that can be configured for either classifi-

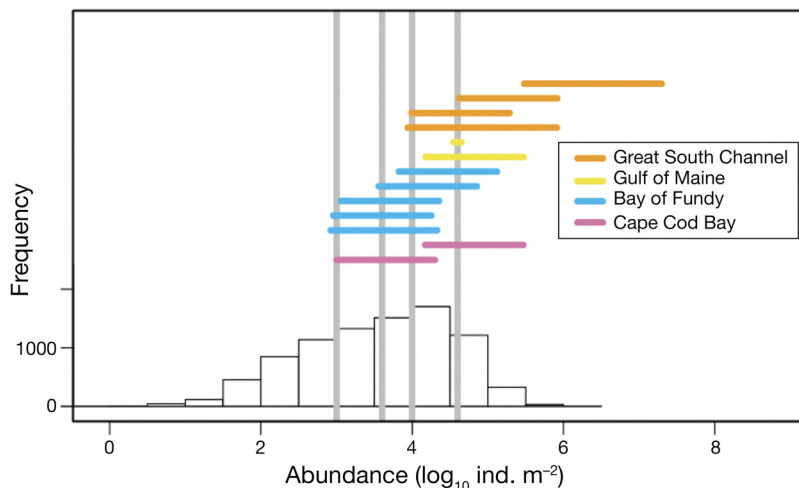


Fig. 2. Abundance of *Calanus finmarchicus* (\log_{10} ind. m^{-2}) from 2000 to 2017 for the unstaged National Oceanic and Atmospheric Administration (NOAA) Fisheries Ecosystem Monitoring Program (MARMAP/EcoMon) dataset. Gray vertical lines indicate the 4 different τ -patch formation thresholds used in this study ($\tau = 1000, 4000, 10\,000,$ and $40\,000$ ind. m^{-2} , respectively). Horizontal bars show *Eubalaena glacialis* feeding thresholds surveyed in the literature review (see Table 2). The 'Gulf of Maine' locations include various sites reported in Baumgartner et al. (2017) and Record et al. (2019) (see Table 2)

cation (i.e. this study) or regression problems. The model consists of a series of decision trees and bootstraps data to avoid convergence issues associated with similar techniques (e.g. classification and regression trees) (Breiman 2001, Evans et al. 2011). Area under the receiver operating characteristic curve (AUC) and the true skill statistic (TSS) were computed for the random forests using inbuilt *bio-mod2* functions and were used to evaluate model performance. Both metrics are methods commonly used to evaluate species distribution models (Fielding & Bell 1997, Allouche et al. 2006, Liu et al. 2011, Ross et al. 2021). AUC and TSS both examine a given model's classification performance using the proportion of true positives. AUC is computed on a scale from 0 to 1, where a value above 0.5 indicates better performance than a random model (Fielding & Bell 1997). TSS is computed on a scale of -1 to 1, where a value of 0 indicates better performance than a random model (Allouche et al. 2006). Interannual trends were computed across the model results in the 5 regional polygons (Fig. 1). A linear regression was performed for each month to assess interdecadal trends in τ -patches over the study period. Environmental covariates were screened to prevent collinearity in the models. For example, if 2 covariates were highly correlated ($r > 0.8$) then the covariate known to have a mechanistic link with *C. finmarchicus* aggregation was retained during the model selection process (e.g. Russo et al. 2015, Bosso et al. 2018). We ran random forest models

both with the entire dataset (using DoY as a covariate; hereafter referred to as the 'whole-year' method), and as 12 individual monthly climatological models. Running the model with 4 thresholds, 2 stage delineations, and whole-year and monthly methods produced 16 final random forest models. We also ran ensembles of generalized additive models, boosted regression trees, and random forest models, for a total of 48 model configurations (Fig. 3). Here, we present the highest performing configuration, based on AUC, with the most plausible habitat maps—the random forest model, using the unstaged data sampled with a mesh size theoretically equivalent to the filtering efficiency of right whale baleen (Mayo et al. 2001), and using DoY as a covariate (i.e. whole-year method).

3. RESULTS

The unstaged EcoMon data comprised a total of 8729 *Calanus finmarchicus* abundance observations, with a mode around 10 000 ind. m^{-2} . Only a few observations exceeded $\tau = 1\,000\,000$ ind. m^{-2} ($n = 3$; Fig. 2). Just over one-third of the observations exceeded $\tau = 10\,000$ ind. m^{-2} ($n = 3280$, 37.6% of the total; Fig. 2). Fewer than one-quarter of the observations exceeded $\tau = 40\,000$ ind. m^{-2} ($n = 1276$, 14.6% of the total; Fig. 2). Feeding threshold values (τ) estimated from the literature spanned the upper portion of the distribution with some regional clustering; estimates from Cape Cod Bay and the Bay of Fundy were lower than in the Great South Channel (Fig. 2). The highest estimated upper-bound threshold from the literature ($20\,000\,000$ m^{-2} , estimated from Kenney et al. 1986; Table 2) exceeded the upper bound represented in the EcoMon dataset.

Qualitative examination of the presence and absence of τ -patches in the EcoMon data showed a clear spatial pattern and seasonality, as well as significant data gaps (Fig. 4). For example, for a threshold of $\tau = 10\,000$ ind. m^{-2} , the presence of τ -patches appeared qualitatively to reach a minimum in February, followed by an increase in the Gulf of Maine and along the continental slope through the spring and summer, with the exception of coastal areas. There was a contraction into the deeper basins of the Gulf of Maine in

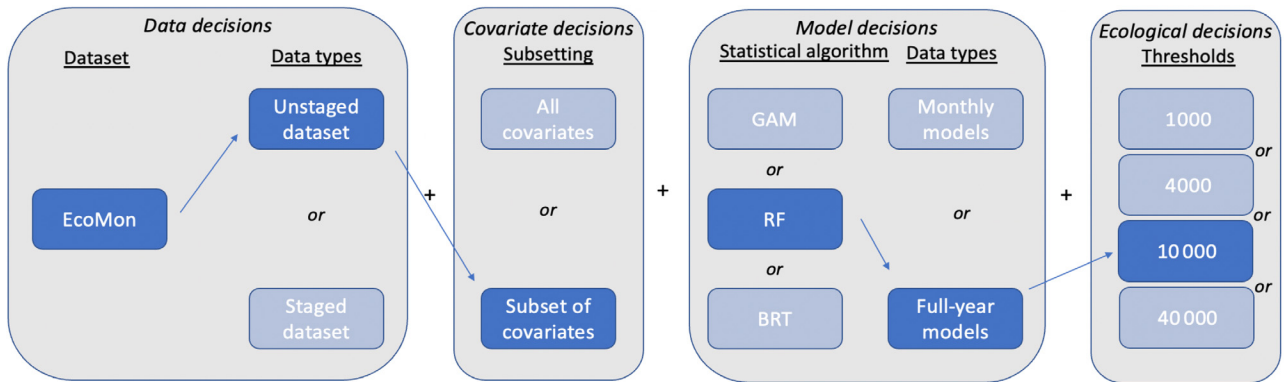


Fig. 3. Modeling decisions considered in this study. The dark blue boxes and arrows highlight the configuration presented with the unstaged dataset, covariates selected based on correlation analysis, the random forest algorithm, and $\tau = 10\,000 \text{ ind. m}^{-2}$

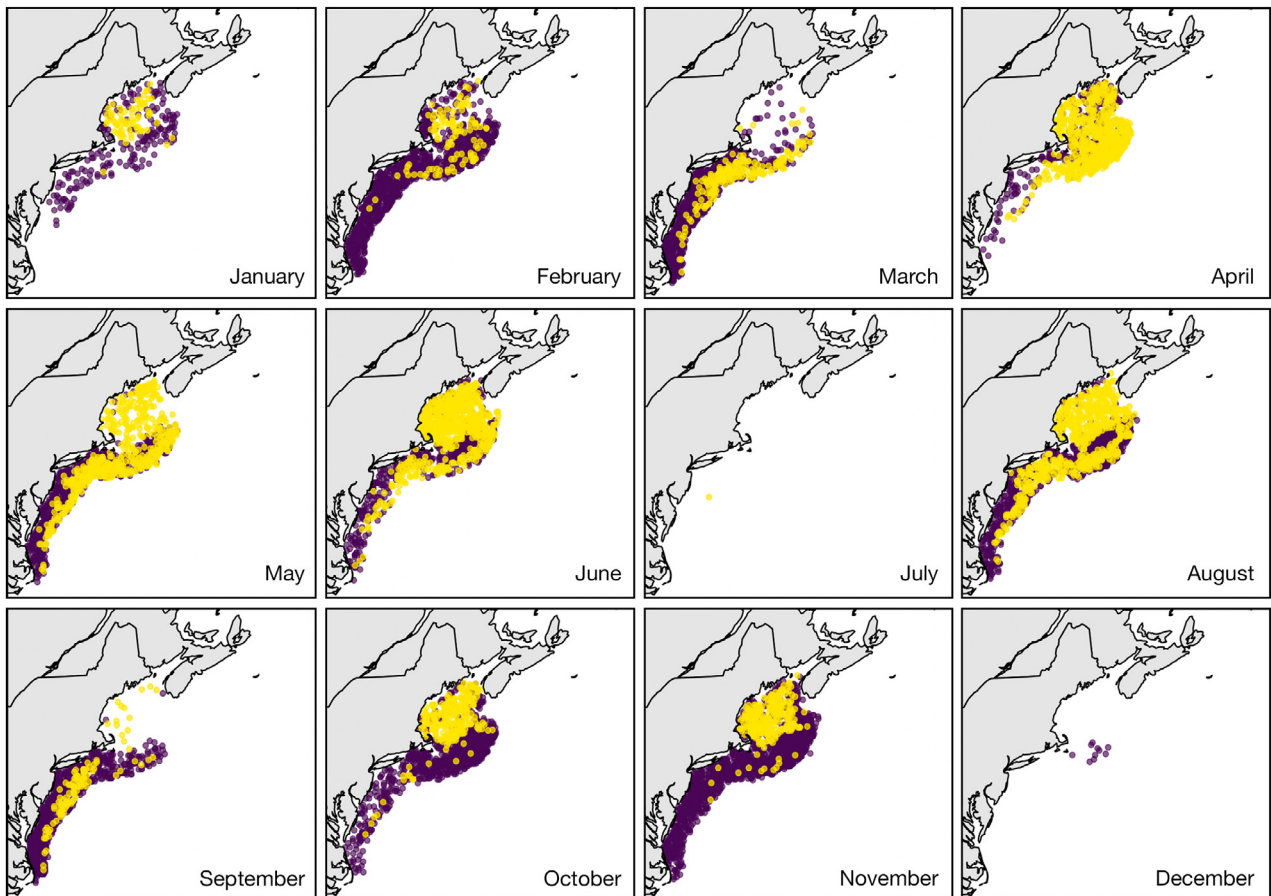


Fig. 4. Monthly presence (yellow points) or absence (purple points) of τ -patches from 2000 to 2017 for a threshold of $\tau = 10\,000 \text{ m}^{-2}$ using the unstaged National Oceanic and Atmospheric Administration (NOAA) Fisheries Ecosystem Monitoring Program (MARMAP/EcoMon)

late summer and fall and a decline in the winter. There was also high τ -patch occurrence along the continental shelf break. The data gap in July and December, as well as in the Gulf of Maine for March and September, highlighted the need for models.

Modeled τ -patch distribution and dynamics matched the seasonal and spatial patterns in the presence/absence of τ -patches in the raw data, which were described in the previous paragraph (Fig. 5). Of the various model configurations tested, the unstaged

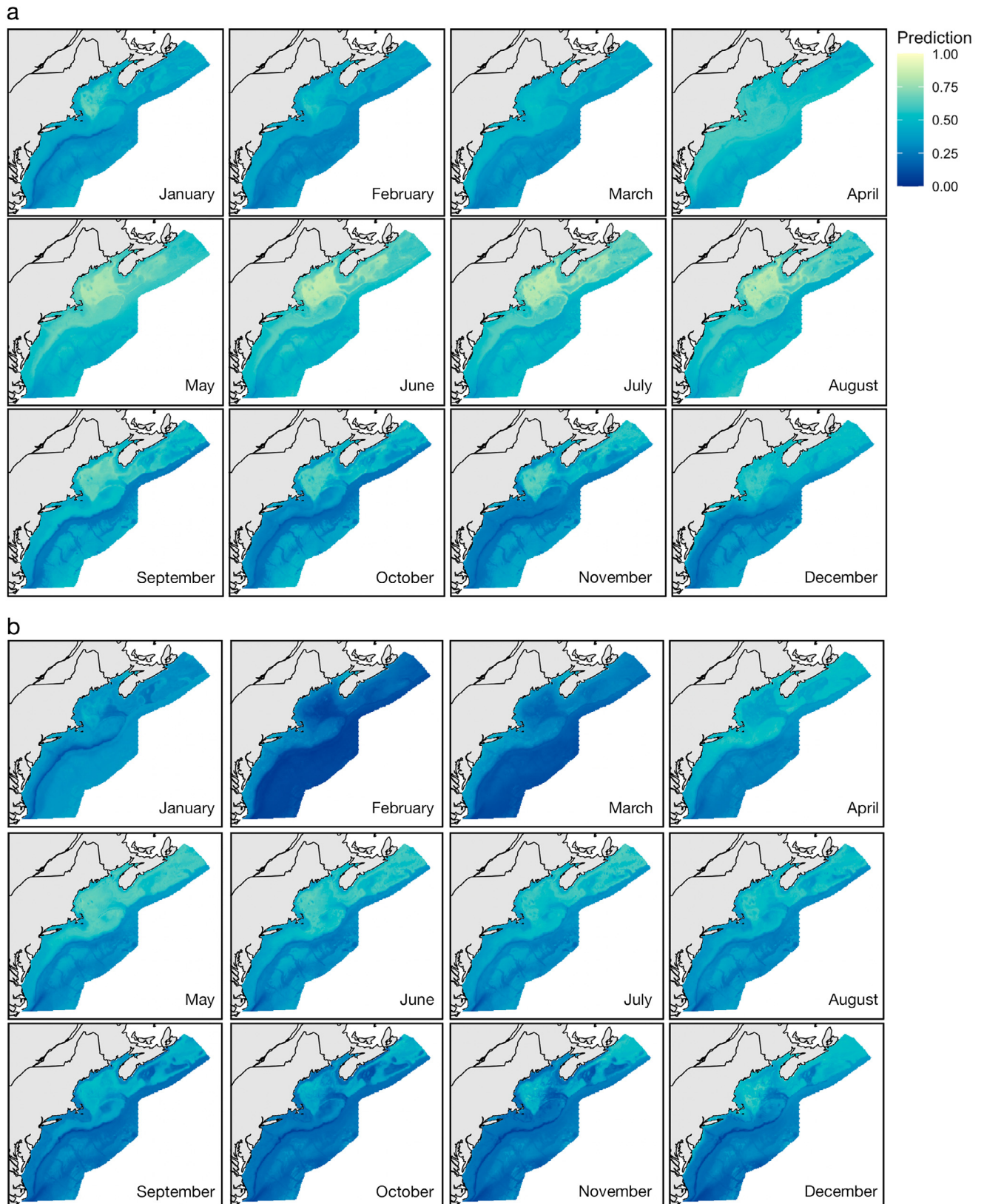


Fig. 5. Projections of *Calanus finmarchicus* τ -patches using thresholds of (a) $\tau = 10\,000$ ind. m^{-2} and (b) $\tau = 40\,000$ ind. m^{-2} for the unstaged National Oceanic and Atmospheric Administration (NOAA) Fisheries Ecosystem Monitoring Program (MARMAP/EcoMon) dataset

Table 3. Model performance for 4 versions of the random forest model evaluated using area under the receiver operating characteristic curve (AUC) and the true skill statistic (TSS). AUC is computed on a 0 to 1 scale (\pm SE). TSS is computed on a -1 to 1 scale (\pm SE). With both metrics, a higher score indicates better model performance

Model version	AUC	TSS
1000 ind. m ⁻² unstaged	0.915 \pm 0.00141	0.6737 \pm 0.00304
4000 ind. m ⁻² unstaged	0.919 \pm 0.00126	0.6887 \pm 0.00353
10 000 ind. m ⁻² unstaged	0.925 \pm 0.00187	0.705 \pm 0.00414
40 000 ind. m ⁻² unstaged	0.907 \pm 0.00171	0.682 \pm 0.00355

data with a threshold of $\tau = 10\,000$ ind. m⁻² using the whole-year method performed the best based on both metrics (Table 3), so most of the results shown will focus on that configuration. The threshold of $\tau = 40\,000$ ind. m⁻² also performed well and is included in e.g. Fig. 5b. In both models, there is a seasonal minimum in February, an increase through the spring and summer, and a contraction into the deep basins in the fall (Fig. 5). In contrast to models of *C. finmarchicus* abundance, the spatial distributions have a high degree of variability that follows bathymetric and oceanographic features; this is often re-

ferred to as prey ‘patchiness’. This variability is particularly pronounced for the $\tau = 40\,000$ ind. m⁻² model (Fig. 5b). EcoMon data do not extend off the continental shelf, so it is difficult to validate the model extrapolation into this habitat. However, the moderate values off the shelf in some months are probably unrealistic, as this is generally not *C. finmarchicus* habitat.

The gaps in the EcoMon data make it difficult to determine trends in τ -patches over time (Fig. 6a). Modeled τ -patch fields allowed us to interpolate these data gaps, giving one way to estimate whether feeding habitats are becoming better or worse over time. We computed trends for each month at each of the 5 *E. glacialis* habitats outlined in Fig. 1 (i.e. Cape Cod Bay, Massachusetts Bay, the Great South Channel, Jordan Basin, and Wilkinson Basin). Trends were significant in certain months using the $\tau = 10\,000$ ind. m⁻² threshold model in the deep basins of the Gulf of Maine (i.e. Jordan Basin and Wilkinson Basin; Fig. 6b). In May, the trends were positive, indicating an increase from 2000 to 2017 in Jordan Basin ($r = 0.704$, $p = 0.00111$) and Wilkinson Basin ($r = 0.772$, $p < 0.001$). In August, the trends were negative in Jordan Basin ($r = -0.648$, $p = 0.00364$) and Wilkinson Basin ($r =$

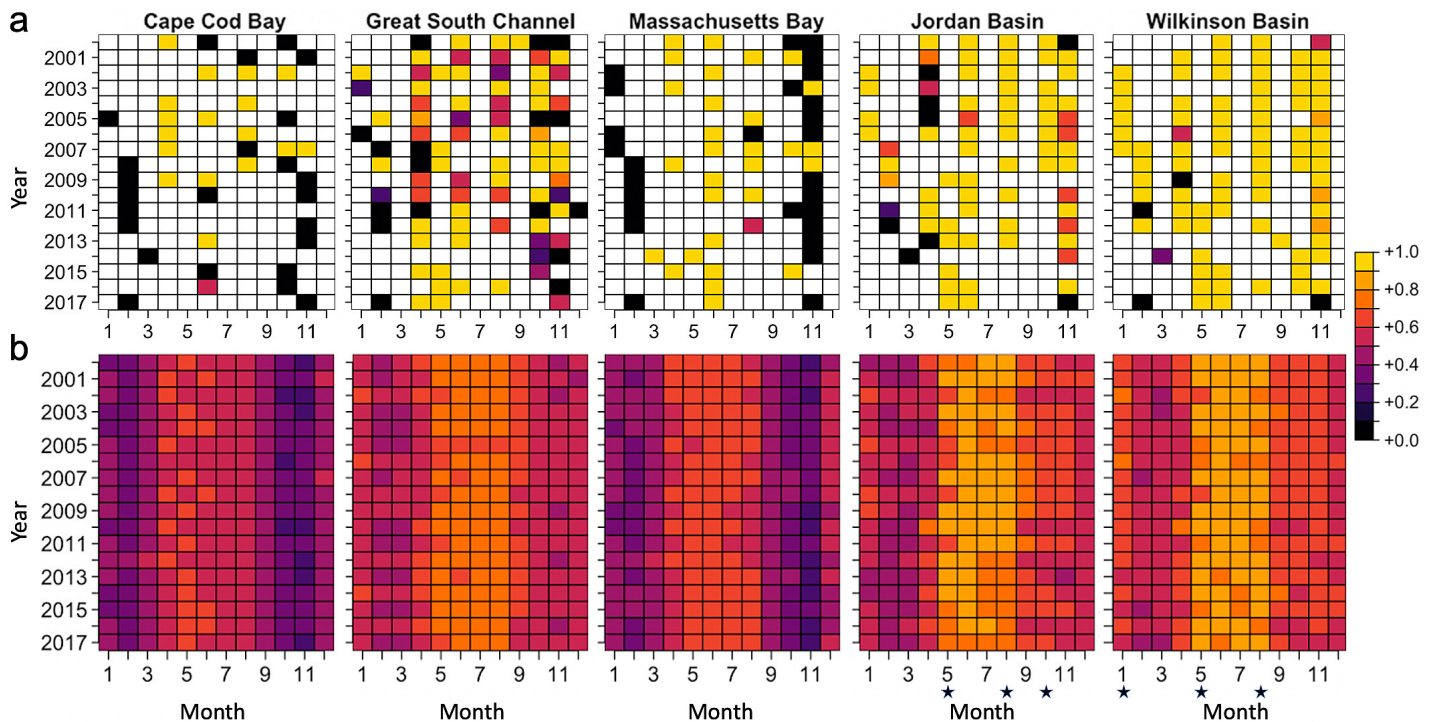


Fig. 6. (a) Plots of the proportion of abundances that exceeded a threshold value of $\tau = 10\,000$ ind. m⁻² for the unstaged National Oceanic and Atmospheric Administration (NOAA) Fisheries Ecosystem Monitoring Program (MARMAP/EcoMon) data. (b) Plots of the prediction of patch formation from the random forest model for a threshold value of $\tau = 10\,000$ ind. m⁻² on a 0 to 1 scale. A star under the x-axis label indicates trends for that month were significant in a given region

-0.657 , $p = 0.00303$). In October, the trend was negative in Jordan Basin ($r = -0.733$, $p = 0.000543$). Trends were similar for the $\tau = 40000 \text{ ind. m}^{-2}$ in the deep basins in May and August, as well. Positive trends were found in May and negative trends were found in August in the deep basins. In October, the trend was negative in Wilkinson Basin ($r = -0.607$, $p = 0.00754$). No significant trends were found in Cape Cod Bay, Massachusetts Bay, or the Great South Channel.

Modeled τ -patch likelihoods matched measured frequencies well, with some notable differences depending on the value of τ . Comparing models and data requires some data binning so that both values fall along a continuous scale from 0 to 1. For comparison, we binned both by month and year, resulting in scatter plots with 216 points (Fig. 7). There were correlations for every selected value of τ . Modeled values tended to overestimate for low probabilities of a τ -patch and match the one-to-one line better for high

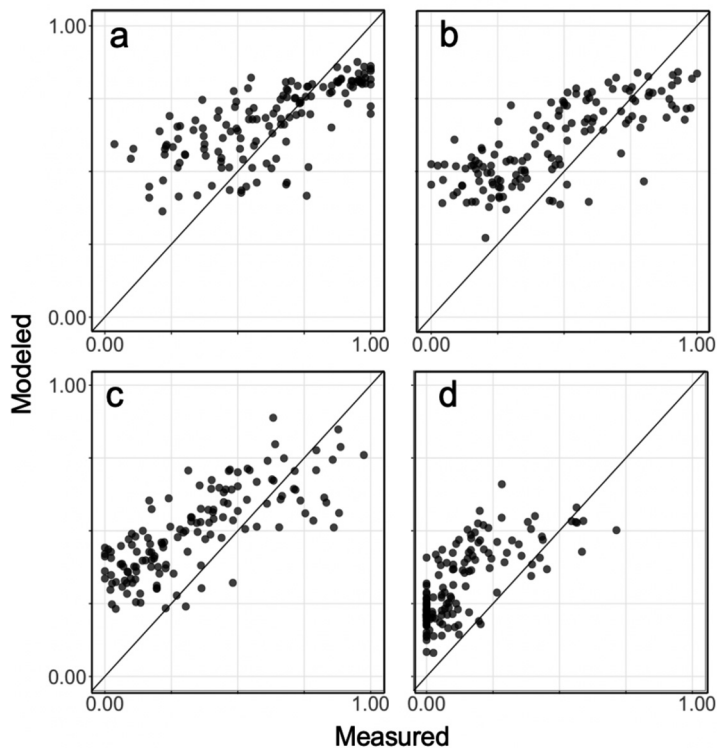


Fig. 7. Measured probability of a high-density τ -patch versus the modeled probability of a τ -patch for (a) $\tau = 1000 \text{ ind. m}^{-2}$ ($r^2 = 0.49$), (b) $\tau = 4000 \text{ ind. m}^{-2}$ ($r^2 = 0.58$), (c) $\tau = 10000 \text{ ind. m}^{-2}$ ($r^2 = 0.63$), and (d) $\tau = 40000 \text{ ind. m}^{-2}$ ($r^2 = 0.49$) for the unstaged National Oceanic and Atmospheric Administration (NOAA) Fisheries Ecosystem Monitoring Program (MARMAP/EcoMon) dataset at a significance level of $p < 0.001$. Points were averaged spatially, with one data point per month per year ($n = 216$). The black line shows the theoretical one-to-one line

probabilities. The strongest correlation was for $\tau = 10000 \text{ ind. m}^{-2}$.

Monthly model runs allowed us to tease apart the covariate contributions to the model and model performance by time of year. Covariate contributions varied seasonally, but bathymetry was consistently the strongest contributor (Fig. 8). From late summer through winter, bottom oceanography had a large contribution. The combined effects of deep-water properties (i.e. bottom temperature and salinity) was a strong contributor in the late summer and fall, consistently stronger than sea surface temperature during this period. In winter months, bottom salinity was the second strongest contributor (behind bathymetry). By contrast, the contribution by surface processes (sea surface temperature, surface temperature gradient, wind, time-integrated surface chlorophyll, and current velocity gradient) peaked in March and April. Time-integrated surface chlorophyll was the second strongest predictor (behind bathymetry) in these months. The seasonal shift between contributions by surface versus bottom covariates aligned with the seasonal life history strategy of *C. finmarchicus*, with deep-water diapause in late summer through winter, and emergence and reproduction following from the spring phytoplankton bloom. The monthly models were unable to run in July and December due to data gaps as a result of under-sampling. Model performance varied seasonally, as well, with AUC generally exceeding a value of 0.8 throughout the year.

Focusing again on the whole-year $\tau = 10000 \text{ ind. m}^{-2}$ model, response curves generally showed unimodal responses across all covariates (Fig. 9). The strong seasonality was reflected in the modeled response to the DoY covariate, which helped to interpolate across the data gaps in July and December. For most covariates, the full scope of the model falls within the well-sampled range of data, with the exception of bathymetry. High bathymetry regions (i.e. deep, off-shelf waters) were undersampled, leading to model extrapolation that was probably unrealistically high where the sample representation dropped off. Model cross-validation runs matched each other closely, particularly where sampling was high.

4. DISCUSSION

Management of *Eubalaena glacialis* could likely be improved by the incorporation of prey information into models and decision support tools (Pendleton et

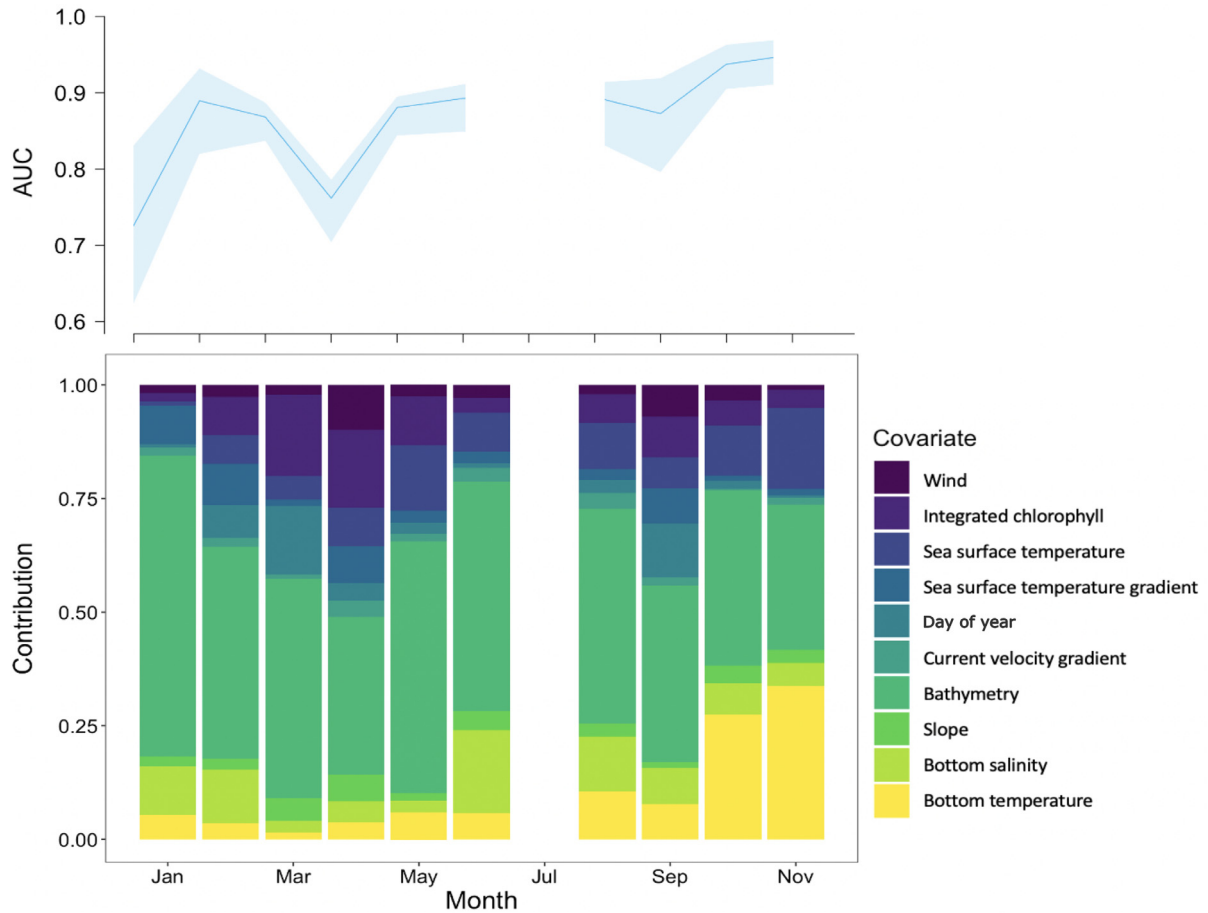


Fig. 8. Monthly covariate contributions with the corresponding model evaluations shown in the top panel. Shaded regions indicate the minimum and maximum area under the receiver operating characteristic curve (AUC) values of the 10 cross-validation runs for a given month

al. 2012, Brennan et al. 2021, Ross et al. 2021). However, there is a disconnect between knowledge of *Calanus finmarchicus* population dynamics and the need for finer-scale information on the high-density copepod aggregations that *E. glacialis* requires. Models and analysis do not generally capture the high-abundance end of the *C. finmarchicus* distribution, which does not necessarily track with overall abundance patterns because of oceanographic and biological processes operating at different spatial and temporal scales.

We modeled the spatiotemporal patterns of τ -patches to better understand their dynamics and develop products for incorporating these dynamics into decision support tools. This required exploring a threshold value, τ , that defined a prey density high enough to attract *E. glacialis* feeding. Empirical critical feeding thresholds reported in the literature vary widely (Table 2), which is not surprising because of the many factors that could influence foraging decisions. A full picture of τ would show monthly, inter-

annual, and possibly regional variability. Understanding how τ varies depending on changing conditions represents an important next step in the prediction of *E. glacialis* movements.

At a high level, τ -patch dynamics, particularly those at the $\tau = 10\,000 \text{ ind. m}^{-2}$ and $40\,000 \text{ ind. m}^{-2}$ levels, followed documented patterns in *E. glacialis* movements during the times of year when whales feed on *C. finmarchicus*. The absence of late summer *C. finmarchicus* abundances exceeding $40\,000 \text{ m}^{-2}$ in Jordan Basin after 2010, for example, matched the timing of the decline of *E. glacialis* use of the eastern Gulf of Maine as a foraging ground (Fig. A1 in the Appendix) (Record et al. 2019). One notable feature of the τ -patch model is that there is finer scale spatial variability than with *C. finmarchicus* abundance models, which are generally much smoother in space (e.g. Pershing et al. 2009a, Reygondeau & Beaugrand 2011, Grieve et al. 2017). This could provide added information for predicting foraging decisions made by *E. glacialis*. Certain features were picked up by

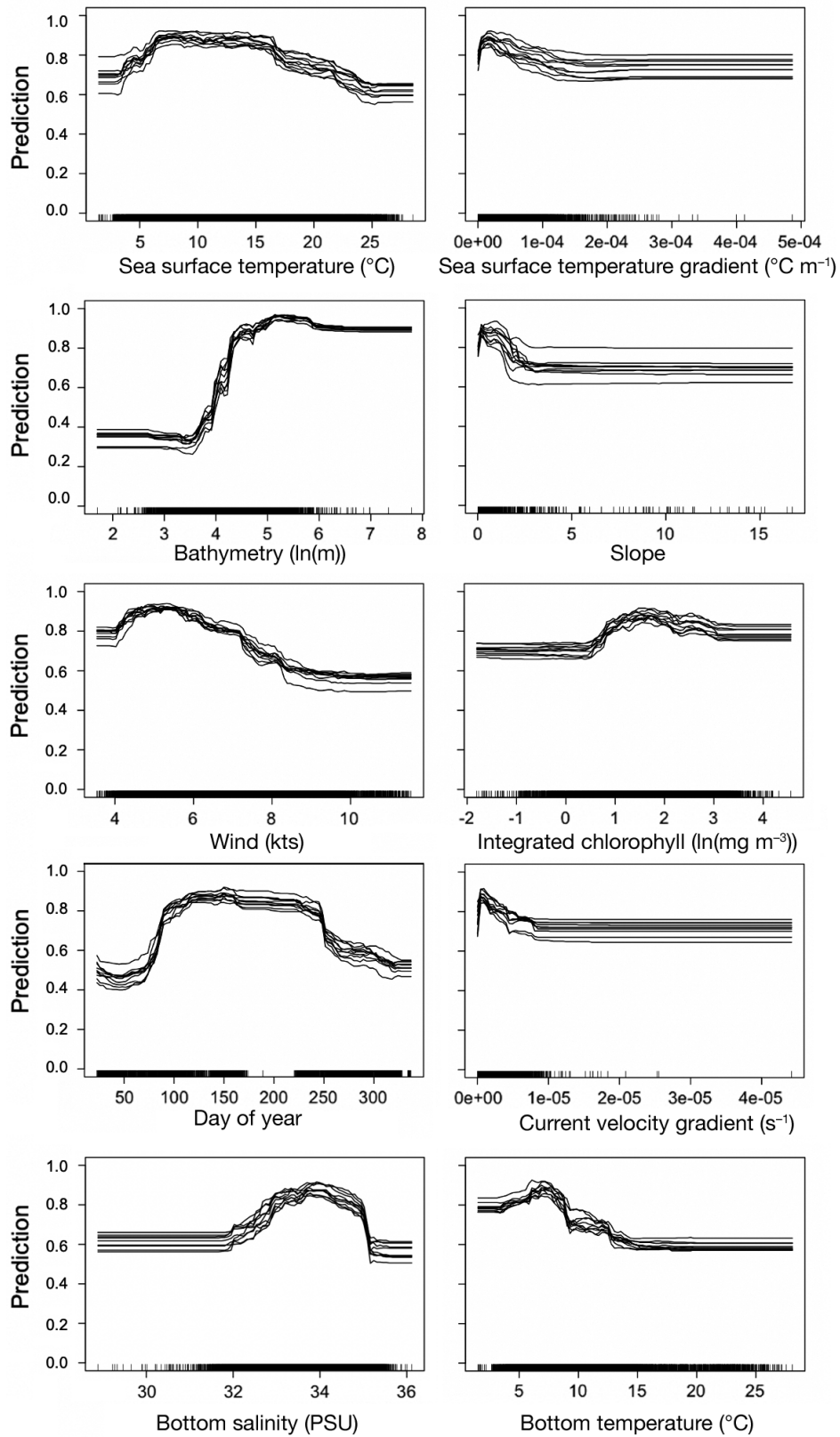


Fig. 9. Response curves for the model with a threshold of $\tau = 10\,000 \text{ ind. m}^{-2}$ with the unstaged National Oceanic and Atmospheric Administration (NOAA) Fisheries Ecosystem Monitoring Program (MARMAP/EcoMon) data. Each line represents one of 10 cross-validation folds

the τ -patch models, such as the higher values along the edge of the continental shelf; this feature appears in the EcoMon data but is not captured by smoother abundance models. This patchy spatial pattern is more pronounced the further toward the high end of the distribution τ is, especially at $\tau = 40\,000 \text{ ind. m}^{-2}$. It is an encouraging indication that modeling τ -patches could be a helpful approach to understand the foraging patterns of *E. glacialis*.

There are some notable differences between the τ -patches and *C. finmarchicus* abundance in covariate associations when comparing with previous statistical models. For example, the favorable sea surface temperature range of *C. finmarchicus* statistically estimated by published models has ranged from 4.5–8.5°C (Reygondeau & Beaugrand 2011) to 6–10°C (Helaouët & Beaugrand 2007). In contrast, the highest τ -patch probabilities in our model occurred for sea surface temperatures of 7–15°C (Fig. 9). Similarly, modeled estimates using bottom temperatures have found peaks at <2°C (Grieve et al. 2017), whereas τ -patch probabilities peaked at bottom temperatures of 4–8°C (Fig. 9). The tendency for high density patches to occur at temperatures warmer than the typical thermal range determined through an abundance model illustrates an advantage of using the τ -patch modeling framework. Unlike the τ -patch framework, a prey abundance model does not tend to predict high abundances in regions with higher sea surface temperatures; these results suggest that τ -patches can occur in these higher temperature regions.

One modeling choice we examined was whether to use unstaged (i.e. all *C. finmarchicus* stages) or staged data (i.e. only stages C4 through adult). We chose to display the models using unstaged data because the mesh size of the EcoMon survey net reflects the filtering capabilities of *E. glacialis* baleen (Mayo et al. 2001). However, focusing on later stages captures the most energetically advantageous *C. finmarchicus* (Mayo et al. 2001, Baumgartner et al. 2003), due to the variations in caloric content with life stage. The performance of these 2 model configurations was very close, with the unstaged configuration performing only slightly better. While the difference was minimal for the EcoMon dataset, this is a consideration that should be carried forward, depending on the sampling method of the dataset used to model τ -patches.

The model here does not fully represent the complex mechanisms underlying τ -patch formation. Even mechanistic bio-physical coupled models do not yet capture the fine-resolution processes at the scales of right whale feeding such as Langmuir circulation and

tidal fronts, although models are improving (e.g. Brennan et al. 2019). Nevertheless, the statistical distribution of *in situ* samples of copepods does capture the occurrence of dense aggregations. Random forests are highly accurate predictive species distribution models (Li & Wang, 2013), and they are able to accurately predict the probability of *C. finmarchicus* τ -patches at the scales examined. Linking the empirical associations of τ -patches with ultra-fine-scale mechanistic models represents an important area of future work that could improve maps of *E. glacialis* prey distribution. Key next steps include coupling to vertically resolved data and models (Plourde et al. 2019, Brennan et al. 2021) and linking models across the full international domain of *E. glacialis* foraging.

The ultimate goal of this work was to provide prey information that could be used in decision support tools for *E. glacialis* management. The next step is to link these modeled prey fields to the right whale modeling used to support decision making (Roberts et al. 2016).

There are some important caveats to note when using of this model. First, *C. finmarchicus* is not the only prey resource for *E. glacialis*. In the winter months, in particular, whales are foraging on smaller copepods, such as *Centropages* spp. and *Pseudocalanus* spp., and there could be other opportunistic prey, such as barnacle larvae (Mayo & Marx 1990). In these cases, dense aggregations also appear to attract whales, so a similar modeling approach could be used; however, τ values and covariate associations are likely to be very different. Second, the EcoMon dataset has no measurements off the northeastern US continental shelf, so using this model to extrapolate into waters deeper than 500 m has very high uncertainty. We chose to show the full projected results for transparency, but we advise cropping this area before incorporating these prey fields into other models, as the projections do not match the expectation for this part of the domain. Finally, the EcoMon data, while being the most extensive dataset for the domain, do not contain information on the vertical distribution of copepods. We were able to constrain the problem by establishing a framework and testing a range of assumptions for vertical distribution, but further refinements of this approach will require blending with vertical distribution data (e.g. Lehoux et al. 2020).

Management of North Atlantic right whales has become increasingly urgent, and the challenge of predicting their movements has been a significant impediment (Davies & Brillant 2019). Much of the whales' movements are guided by their prey, and new approaches to incorporating prey information

into decision support promise to be helpful. A closer look at the dynamics of the highest-density aggregations of prey gives a new lens to an old problem and could provide another tool for helping to predict right whale movements.

Data availability. The computed τ -patch fields are available from the corresponding author (C. H. Ross) upon request.

Acknowledgements. We thank those who participated in collecting the National Oceanic and Atmospheric Administration (NOAA) Fisheries Ecosystem Monitoring Program (MARMAP/EcoMon) data and Harvey Walsh for providing updated data and species stage information. We thank Daniel E. Pendleton, Kimberly T. A. Davies, and 3 anonymous reviewers for their feedback on this manuscript. This work was funded by NOAA grant NA20NMF0080246, MBON grant NA19NOS0120197, BOEM Cooperative Agreement M19AC00022, the Maine Community Foundation, Tandy Center for Ocean Forecasting institutional funds, and Bigelow Laboratory for Ocean Sciences institutional funds.

LITERATURE CITED

- Allouche O, Tsoar A, Kadmon R (2006) Assessing the accuracy of species distribution models: prevalence, kappa, and the true skill statistic (TSS). *J Appl Ecol* 43:1223–1232
- Baumgartner MF, Mate BR (2003) Summertime foraging ecology of North Atlantic right whales. *Mar Ecol Prog Ser* 264:123–135
- Baumgartner MF, Cole TVN, Clapham PJ, Mate BR (2003) North Atlantic right whale habitat in the lower Bay of Fundy on the SW Scotian Shelf during 1999–2001. *Mar Ecol Prog Ser* 264:137–154
- Baumgartner MF, Wenzel FW, Lysiak NSJ, Patrician MR (2017) North Atlantic right whale foraging ecology and its role in human-caused mortality. *Mar Ecol Prog Ser* 581:165–181
- Beardsley RC, Epstein AW, Chen CS, Wishner KF, Macaulay MC, Kenney RD (1996) Spatial variability in zooplankton abundance near feeding right whales in the Great South Channel. *Deep Sea Res II* 43:1601–1625
- Bosso L, Smeraldo S, Rapuzzi P, Sama G, Garonna AP, Russo D (2018) Nature protection areas of Europe are insufficient to preserve the threatened beetle *Rosalia alpina* (Coleoptera: Cerambycidae): evidence from species distribution models and conservation gap analysis. *Ecol Entomol* 43:192–203
- Breiman L (2001) Random forests. *Mach Learn* 45:5–32
- Brennan CE, Maps F, Gentleman WC, Plourde S and others (2019) How transport shapes copepod distributions in relation to whale feeding habitat: demonstration of a new modelling framework. *Prog Oceanogr* 171:1–21
- Brennan CE, Maps F, Gentleman WC, Lavoie D, Chassé J, Plourde S, Johnson CL (2021) Ocean circulation changes drive shifts in *Calanus* abundance in North Atlantic right whale foraging habitat: a model comparison of cool and warm year scenarios. *Prog Oceanogr* 197:102629
- CETAP (Cetacean and Turtle Assessment Program) (1982) A characterization of marine mammals and turtles in the mid-and North Atlantic areas of the U.S. outer continental shelf. Final report, contract no. AA551-CT8–48, Bureau of Land Management, Washington, DC
- Chust G, Castellani C, Licandro P, Ibiabarraiga L, Sagarmina Y, Irigoien X (2014) Are *Calanus* spp. shifting poleward in the North Atlantic? A habitat modelling approach. *ICES J Mar Sci* 71:241–253
- Cooke JG (2020) *Eubalaena glacialis* (errata version published in 2020). IUCN Red List Threat Anim 2020: e.T41712A178589687
- Davies KTA, Brillant SW (2019) Mass human-caused mortality spurs federal action to protect endangered North Atlantic right whales in Canada. *Mar Policy* 104:157–162
- Davies KTA, Taggart CT, Smedbol RK (2014) Water mass structure defines the diapausing copepod distribution in a right whale habitat on the Scotian Shelf. *Mar Ecol Prog Ser* 497:69–85
- Davis GE, Baumgartner MF, Bonnell JM, Bell J and others (2017) Long-term passive acoustic recordings track the changing distribution of North Atlantic right whales (*Eubalaena glacialis*) from 2004 to 2014. *Sci Rep* 7:13460
- Epstein AW, Beardsley RC (2001) Flow-induced aggregation of plankton at a front: a 2-D Eulerian model study. *Deep Sea Res II* 48:395–418
- Evans JS, Murphy MA, Holden ZA, Cushman SA (2011) Modeling species distribution and change using random forest. In: Drew CA, Wiersma YF, Huettmann F (eds) Predictive species and habitat modeling in landscape ecology: concepts and applications. Springer, New York, NY, p 139–159
- Fielding AH, Bell JF (1997) A review of methods for the assessment of prediction errors in conservation presence/absence models. *Environ Conserv* 24:38–49
- Fortune SME, Trites AW, Mayo CA, Rosen DAS, Hamilton PK (2013) Energetic requirements of North Atlantic right whales and the implications for species recovery. *Mar Ecol Prog Ser* 478:253–272
- Friedland KD, Morse RE, Manning JP, Melrose DC and others (2020) Trends and change points in surface and bottom thermal environments of the US Northeast Continental Shelf Ecosystem. *Fish Oceanogr* 29:396–414
- Gonçalves Neto A, Langan JA, Palter JB (2021) Changes in the Gulf Stream preceded rapid warming of the Northwest Atlantic Shelf. *Nat Commun Earth Environ* 2:74
- Grieve BD, Hare JA, Saba VS (2017) Projecting the effects of climate change on *Calanus finmarchicus* distribution within the U.S. Northeast Continental Shelf. *Sci Rep* 7: 6264
- Helaouët P, Beaugrand G (2007) Macroecology of *Calanus finmarchicus* and *C. helgolandicus* in the North Atlantic Ocean and adjacent seas. *Mar Ecol Prog Ser* 345:147–165
- Ji R (2011) *Calanus finmarchicus* diapause initiation: new view from traditional life history-based model. *Mar Ecol Prog Ser* 440:105–111
- Ji R, Feng Z, Jones BT, Thompson C, Chen C, Record NR, Runge JA (2017) Coastal amplification of supply and transport (CAST): a new hypothesis about the persistence of *Calanus finmarchicus* in the Gulf of Maine. *ICES J Mar Sci* 74:1865–1874
- Ji R, Runge JA, Davis CS, Wiebe PH (2022) Drivers of variability of *Calanus finmarchicus* in the Gulf of Maine: roles of internal production and external exchange. *ICES J Mar Sci* 79:775–784
- Jiang M, Brown MW, Turner JT, Kenney RD, Mayo CA, Zhang Z, Zhou M (2007) Springtime transport and retention of *Calanus finmarchicus* in Massachusetts and Cape

- Cod Bays, USA, and implications for right whale foraging. *Mar Ecol Prog Ser* 349:183–197
- Kane J (2007) Zooplankton abundance trends on Georges Bank, 1977–2004. *ICES J Mar Sci* 64:909–919
- Kann LM, Wishner K (1995) Spatial and temporal patterns of zooplankton on baleen whale feeding grounds in the southern Gulf of Maine. *J Plankton Res* 17:235–262
- Kenney RD, Wishner KF (1995) The South Channel Ocean Productivity Experiment. *Cont Shelf Res* 15:373–384
- Kenney RD, Hyman MAM, Owen RE, Scott GP, Winn HE (1986) Estimation of prey densities required by western North Atlantic right whales. *Mar Mamm Sci* 2:1–13
- Kraus SD, Kenney RD, Mayo CA, McLellan WA, Moore MJ, Nowacek DP (2016) Recent scientific publications cast doubt on North Atlantic right whale future. *Front Mar Sci* 3:137
- Lehoux C, Plourde S, Lesage V (2020) Significance of dominant zooplankton species to the North Atlantic right whale potential foraging habitats in the Gulf of St. Lawrence: a bio-energetic approach. DFO Canadian Science Advisory Secretariat Research Document, 2020/033
- Li X, Wang Y (2013) Applying various algorithms for species distribution modeling. *Integr Zool* 8:124–135
- Liu C, White M, Newell G (2011) Measuring and comparing the accuracy of species distribution models with presence-absence data. *Ecography* 34:232–243
- Lynch DR, Gentleman WC, McGillicuddy DJ Jr, Davis CS (1998) Biological/physical simulations of *Calanus finmarchicus* population dynamics in the Gulf of Maine. *Mar Ecol Prog Ser* 169:189–210
- Mayo CA, Marx MK (1990) Surface foraging behaviour of the North Atlantic right whale, *Eubalaena glacialis*, and associated zooplankton characteristics. *Can J Zool* 68:2214–2220
- Mayo CA, Letcher BH, Scott S (2001) Zooplankton filtering efficiency of the baleen of a North Atlantic right whale, *Eubalaena glacialis*. *J Cetacean Res Manag* 3:245–250
- Mayo CA, Nichols OC, Bessinger MK, Brown MW, Marx MK, Browning CL (2004) Surveillance, monitoring and management of North Atlantic right whales in Cape Cod Bay and adjacent waters — 2004. Final report submitted to the Commonwealth of Massachusetts, Division of Marine Fisheries, Boston, MA
- Meise CJ, O'Reilly JE (1996) Spatial and seasonal patterns in abundance and age composition of *Calanus finmarchicus* in the Gulf of Maine and on Georges Bank 1977–1987. *Deep Sea Res II* 43:1473–1501
- Melle W, Runge J, Head E, Plourde S and others (2014) The North Atlantic Ocean as habitat for *Calanus finmarchicus*: Environmental factors and life history traits. *Prog Oceanogr* 129:244–284
- Meyer-Gutbrod EL, Greene CH, Davies KTA, Johns DG (2021) Ocean regime shift is driving collapse of the North Atlantic right whale population. *Oceanogr Mag* 34:22–31
- Michaud J, Taggart CT (2007) Lipid and gross energy content of North Atlantic right whale food, *Calanus finmarchicus*, in the Bay of Fundy. *Endang Species Res* 3:77–94
- Miller CA, Reeb D, Best PB, Knowlton AR, Brown MW, Moore MJ (2011) Blubber thickness in right whales *Eubalaena glacialis* and *Eubalaena australis* related with reproduction, life history status and prey abundance. *Mar Ecol Prog Ser* 438:267–283
- Murison LD, Gaskin DE (1989) The distribution of right whales and zooplankton in the Bay of Fundy, Canada. *Can J Zool* 67:1411–1420
- Pendleton DE, Pershing AJ, Brown MW, Mayo CA, Kenney RD, Record NR, Cole TVN (2009) Regional-scale mean copepod concentration indicates relative abundance of North Atlantic right whales. *Mar Ecol Prog Ser* 378:211–225
- Pendleton DE, Sullivan PJ, Brown MW, Cole TVN and others (2012) Weekly predictions of North Atlantic right whale *Eubalaena glacialis* habitat reveal influence of prey abundance and seasonality of habitat preferences. *Endang Species Res* 18:147–161
- Pershing AJ, Stamieszkin K (2020) The North Atlantic ecosystem, from plankton to whales. *Annu Rev Mar Sci* 12:339–359
- Pershing AJ, Record NR, Monger BC, Pendleton DE, Woodward LA (2009a) Model-based estimates of *Calanus finmarchicus* abundance in the Gulf of Maine. *Mar Ecol Prog Ser* 378:227–243
- Pershing AJ, Record NR, Monger BC, Mayo CA and others (2009b) Model-based estimates of right whale habitat use in the Gulf of Maine. *Mar Ecol Prog Ser* 378:245–257
- Pershing AJ, Hernandez CM, Kerr LA, LeBris A and others (2015) Slow adaptation in the face of rapid warming leads to the collapse of an iconic fishery. *Science* 350:809–812
- Plourde S, Lehoux C, Johnson CL, Perrin G, Lesage V (2019) North Atlantic right whale (*Eubalaena glacialis*) and its food: (I) a spatial climatology of *Calanus* biomass and potential foraging habitats in Canadian waters. *J Plankton Res* 41:667–685
- Core Team (2021) R: a language and environment for statistical computing. R Foundation for Statistical Computing, Vienna. www.r-project.org
- Record NR, Pershing AJ, Maps F (2013) Emergent copepod communities in an adaptive trait-structured model. *Ecol Model* 260:11–24
- Record NR, Ji R, Maps F, Varpe Ø, Runge JA, Petrik CM, Johns DA (2018) Copepod diapause and the biogeography of the marine lipidscape. *J Biogeogr* 45:2238–2251
- Record NR, Runge JA, Pendleton DE, Balch WM and others (2019) Rapid climate-driven circulation changes threaten conservation of endangered North Atlantic right whales. *Oceanography* 32(2):162–169
- Reygondeau G, Beaugrand G (2011) Future climate-driven shifts in distribution of *Calanus finmarchicus*. *Glob Change Biol* 17:756–766
- Richardson DE, Hare JA, Overholtz WJ, Johnson DL (2010) Development of long-term larval indices for Atlantic herring (*Clupea harengus*) on the northeast US continental shelf. *ICES J Mar Sci* 67:617–627
- Roberts JJ, Best B, Mannocci L, Fujioka E and others (2016) Habitat-based cetacean density models for the U.S. Atlantic and Gulf of Mexico. *Sci Rep* 6:22615
- Roberts JJ, Schick RS, Halpin PN (2020) Final Project Report: Marine Species Density Data Gap Assessments and Update for the AFTT Study Area, 2018–2020 (Option Year 3). Document version 1.4. Report prepared for Naval Facilities Engineering Command, Atlantic by the Duke University Marine Geospatial Ecology Lab, Durham, NC
- Ross CH, Pendleton DE, Tupper B, Brickman D, Zani MA, Mayo CA, Record NR (2021) Projecting regions of North Atlantic right whale, *Eubalaena glacialis*, habitat suitability in the Gulf of Maine for the year 2050. *Elem Sci Anthropocene* 9:00058
- Runge JA, Ji R, Thompson CRS, Record NR and others (2015) Persistence of *Calanus finmarchicus* in the western Gulf

- of Maine during recent extreme warming. *J Plankton Res* 37:221–232
- ✦ Russo D, Di Febbraro M, Cistrone L, Jones G, Smeraldo S, Garonna A, Bosso L (2015) Protecting one, protecting both? Scale-dependent ecological differences in two species using dead trees, the rosalia longicorn beetle and the barbastelle bat. *J Zool (Lond)* 297: 165–175
- ✦ Sorochan KA, Ploudre S, Morse R, Pepin P, Runge JA, Thompson C, Johnson CL (2019) North Atlantic right whales (*Eubalaena glacialis*) and its food: (II) interannual variations in biomass of *Calanus* spp. on western North Atlantic shelves. *J Plankton Res* 41:687–708
- ✦ Sorochan KA, Brennan CE, Plourde S, Johnson CL (2021) Spatial variation and transport of abundant copepod taxa in the southern Gulf of St. Lawrence in autumn. *J Plankton Res* 43:908–926
- Stephens DW, Krebs JR (1986) Foraging theory. Princeton University Press, Princeton, NJ
- ✦ Thuiller W, Lafourcade B, Engler R, Araújo MB (2009) BIO-MOD—A platform for ensemble forecasting of species distributions. *Ecography* 32:369–373
- Wishner K, Durbin E, Durbin A, Macaulay M, Winn H, Kenney R (1988) Copepod patches and right whales in the Great South Channel off New England. *Bull Mar Sci* 43: 825–844
- ✦ Wishner KF, Schoenherr JR, Beardsley R, Chen C (1995) Abundance, distribution and population structure of the copepod *Calanus finmarchicus* in a springtime right whale feeding area in the southwestern Gulf of Maine. *Cont Shelf Res* 15:475–507
- ✦ Woodley TH, Gaskin DE (1996) Environmental characteristics of North Atlantic right and fin whale habitat in the lower Bay of Fundy, Canada. *Can J Zool* 74:75–84

Appendix.

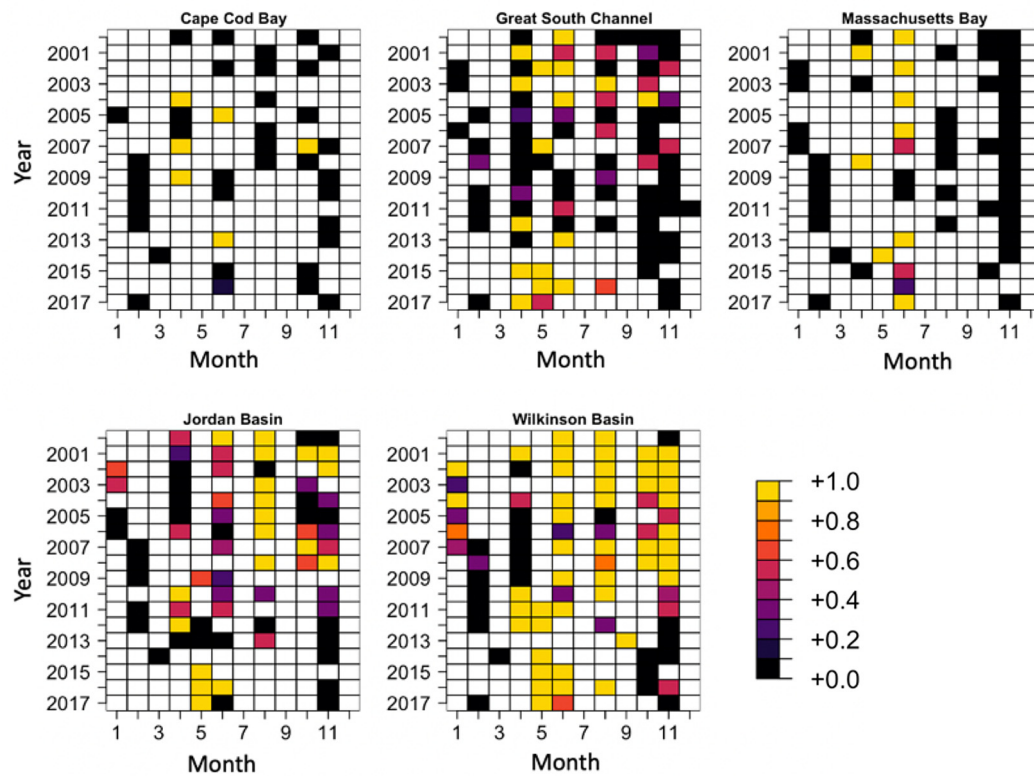


Fig. A1. Plots of the proportion of abundances that exceeded a threshold value of $\tau = 40,000 \text{ ind. m}^{-2}$ for the unstaged National Oceanic and Atmospheric Administration (NOAA) Fisheries Ecosystem Monitoring Program (MARMAP/EcoMon) data

Editorial responsibility: Sigrun Jónasdóttir,
Charlottenlund, Denmark
Reviewed by: 3 anonymous referees

Submitted: April 26, 2022
Accepted: October 28, 2022
Proofs received from author(s): January 10, 2023